

# A concave pairwise fusion approach to subgroup analysis

Shujie Ma\*

Department of Statistics, University of California Riverside  
and

Jian Huang†

Department of Statistics and Actuarial Science, University of Iowa

## Abstract

An important step in developing individualized treatment strategies is to correctly identify subgroups of a heterogeneous population, so that specific treatment can be given to each subgroup. In this paper, we consider the situation with samples drawn from a population consisting of subgroups with different means, along with certain covariates. We propose a penalized approach for subgroup analysis based on a regression model, in which heterogeneity is driven by unobserved latent factors and thus can be represented by using subject-specific intercepts. We apply concave penalty functions to pairwise differences of the intercepts. This procedure automatically divides the observations into subgroups. We develop an alternating direction method of multipliers algorithm with concave penalties to implement the proposed approach and demonstrate its convergence. We also establish the theoretical properties of our proposed estimator and determine the order requirement of the minimal difference of signals between groups in order to recover them. These results provide a sound basis for making statistical inference in subgroup analysis. Our proposed method is further illustrated by simulation studies and analysis of the Cleveland heart disease dataset.

*Keywords:* asymptotic normality; heterogeneity; inference; linear regression; oracle property

*Short title:* Subgroup analysis

---

\*The research of Ma is supported in part by the U.S. NSF grant DMS-13-06972.

†Corresponding author. The research of Huang is supported in part by the U.S. NSF grant DMS-12-08225.

# 1 Introduction

Personalized medicine has gained much attention in the past decade, which emphasizes the use of information available on individual patients to make treatment decisions. Developing individualized treatment strategies requires sophisticated analytic tools. One of the key statistical challenges is to correctly identify subgroups from a heterogeneous population, so that specific medical therapies can be given to each subgroup. A popular method for analyzing data from a heterogeneous population is to view data as coming from a mixture of subgroups with their own sets of parameter values and then use finite mixture model analysis (Everitt and Hand, 1981). The mixture model approach has been widely used for data clustering and classification; see Banfield and Raftery (1993), Hastie and Tibshirani (1996), McNicholas (2010) and Wei and Kosorok (2013) for the Gaussian mixture model approaches, Shen and He (2015) for a logistic-normal mixture model method, and Chaganty and Liang (2013) for a low-rank method for mixtures of linear regressions which provides a good initialization for the EM algorithm typically used in estimation of mixture models. The mixture model-based approach as a supervised clustering method needs to specify an underlying distribution for the data, and it also requires specifying the number of mixture components in the population which is often difficult to do in practice.

In this paper, we propose a new approach to automatically detecting and identifying homogeneous subgroups based on a concave pairwise fusion penalty without the knowledge of an *a priori* classification or a natural basis of separating a sample into subsets. Let  $y_i$  be the response variable for the  $i^{\text{th}}$  subject. After adjusting for the effects of a set of covariates  $\mathbf{x}_i = (x_{i1}, \dots, x_{ip})^T$ , we consider subgroup analysis for  $\mathbf{y} = (y_1, \dots, y_n)^T$  with the heterogeneity driven by unknown or unobserved latent factors, which can be modeled through subject-specific intercepts in regression. Hence, we consider

$$y_i = \mu_i + \mathbf{x}_i^T \boldsymbol{\beta} + \epsilon_i, i = 1, \dots, n, \quad (1)$$

where  $\mu_i$ 's are unknown subject-specific intercepts,  $\boldsymbol{\beta} = (\beta_1, \dots, \beta_p)^T$  is the vector of unknown coefficients for the covariates  $\mathbf{x}_i$ , and  $\epsilon_i$  is the error term independent of  $\mathbf{x}_i$  with  $E(\epsilon_i) = 0$  and  $\text{Var}(\epsilon_i) = \sigma^2$ . For example, in biomedical studies,  $y_i$  can be certain phenotype associated with some disease such as the maximal heart rate which is related to cardiac mortality or

body mass index associated with obesity, and  $\mathbf{x}_i$  is a set of observed covariates such as gender, age, race, etc. After adjusting for the effects of the covariates, the distribution of the response is still heterogeneous, as demonstrated by multiple modes in the density plot shown in Figure 5 for our heart disease application. This heterogeneity can be caused by unobserved latent factors, so that it is modeled through the subject-specific  $\mu_i$ 's.

It is worth noting that if the factors contributing to this heterogeneity, for example, different treatments, become available, then  $\mu_i$  can be written as  $\mu_i = \mu + \mathbf{z}_i^T \boldsymbol{\theta}$ , where  $\mathbf{z}_i$  are the observed variables for the treatments and  $\boldsymbol{\theta}$  are the coefficients of  $\mathbf{z}_i$ . One interesting application in personalized medicine is that the coefficients for  $\mathbf{z}_i$  can be subject-specific, since the same treatment may have different effects on patients. For this case, we can consider the model with heterogeneous effects of some covariates given as

$$y_i = \mu + \mathbf{z}_i^T \boldsymbol{\theta}_i + \mathbf{x}_i^T \boldsymbol{\beta} + \epsilon_i, i = 1, \dots, n. \quad (2)$$

Throughout this paper, we focus on studying model (1) by considering that the heterogeneity comes from unobserved latent factors. However, our proposed estimation method and the associated theoretical properties for model (1) can be extended to model (2) with some modifications. We provide the detailed estimation procedure for model (2) in Section A.4 of the Supplemental Materials for interested readers. Assumptions of the structure are needed in order to estimate model (1). To this end, we assume that  $\mathbf{y} = (y_1, \dots, y_n)^T$  are from  $K$  different groups with  $K \geq 1$  and the data from the same group have the same intercept. In other words, let  $\mathcal{G} = (\mathcal{G}_1, \dots, \mathcal{G}_K)$  be a partition of  $\{1, \dots, n\}$ . We have  $\mu_i = \alpha_k$  for all  $i \in \mathcal{G}_k$ , where  $\alpha_k$  is the common value for the  $\mu_i$ 's from group  $\mathcal{G}_k$ . In practice, the number of groups  $K$  is unknown. However, it is usually reasonable to assume that  $K$  is much smaller than  $n$ . Our goal is to estimate  $K$  and identify the subgroups. We are also interested in estimating the intercepts  $(\alpha_1, \dots, \alpha_K)$  and the regression parameter  $\boldsymbol{\beta}$ . We propose a concave pairwise fusion penalized least squares approach for this purpose and derive an alternating direction method of multipliers (ADMM, Boyd et al (2011)) algorithm for implementing the proposed approach.

Several authors have studied the problem of exploring homogeneity effects of covariates in the regression setting by assuming that the true coefficients are divided into a few clus-

ters with common values. For instance, Tibshirani et al (2005) proposed the fused LASSO method which applies  $L_1$  penalties to the pairs of adjacent coordinates given that a complete ordering of covariates is available. Bondell and Reich (2008) proposed the OSCAR method where a special octagonal shrinkage penalty is applied to each pair of coordinates. Shen and Huang (2010) developed a group pursuit approach with truncated  $L_1$  penalties to the pairwise differences, and Ke et al (2013) proposed a method called CARDS. All the above methods are about estimating homogeneity effects of covariates, which is different from our work aiming to identify subgroups of the observations. Guo et al (2010) proposed using a pairwise  $L_1$  fusion penalty for identifying informative variable in the context of Gaussian model-based cluster analysis. In the unsupervised learning setting, a recent paper (Chi and Lange (2001)) considered the convex clustering problem and investigated the ADMM and the alternating minimization algorithms with the convex  $L_p$  ( $p \geq 1$ ) penalties applied to the pairwise differences of the data points.

The ADMM has good convergence properties for convex loss functions with the  $L_p$ ,  $p \geq 1$ , penalties (Boyd et al (2011) and Chi and Lange (2001)). Moreover, the  $L_1$  penalty can shrink some pairwise differences of the parameter estimates to zero. However, the  $L_1$  penalty generates large biases of the estimates in each iteration of the algorithm. As a result, it may not be able to identify the subgroups, as illustrated in Figure 1. To address this issue, Chi and Lange (2001) propose to multiply nonnegative weights to the  $L_1$  norms to reduce the bias. However, the choice of the weights can dramatically affect the quality of the clustering solution, and there is no clear rule for how to choose the weights. Thus, a penalty which can produce unbiased estimates is more desirable for identifying subgroups. We propose an ADMM algorithm by using concave pairwise fusion penalties for estimation of model (1). The concave penalties in the optimization problem such as the smoothly clipped absolute deviations penalty (SCAD, Fan and Li (2001)) and the minimax concave penalty (MCP, Zhang (2010)) enjoy the unbiasedness property. We then derive the convergence properties of the ADMM algorithm. Moreover, we provide theoretical analysis of the proposed estimators. Specifically, we derive the order requirement of the minimum difference of signals between groups in order to identify the true subgroups. We also establish the oracle property that under mild regularity conditions the oracle estimator is a local minimizer of

the objective function with a high probability. The oracle estimator is obtained from least squares regression by assuming that the true group structure is known.

The rest of this paper is organized as follows. In Section 2 we describe the proposed approach in detail. In Section 3 we derive an ADMM algorithm with concave penalties. We then state the theoretical properties of the proposed approach in Section 4. In Sections 5 we evaluate the finite sample properties of the proposed procedures via simulation studies. Section 6 illustrates the proposed method through a data example. Some concluding remarks are given in Section 7. The estimation procedure for model (2) and all the technical proofs are provided in the on-line Supplemental Materials.

## 2 Subgroup analysis via concave pairwise fusion

For estimation of model (1), we propose a concave pairwise fusion penalized least squares approach. The objective function is

$$Q_n(\boldsymbol{\mu}, \boldsymbol{\beta}; \lambda) = \frac{1}{2} \sum_{i=1}^n (y_i - \mu_i - \mathbf{x}_i^T \boldsymbol{\beta})^2 + \sum_{1 \leq i < j \leq n} p(|\mu_i - \mu_j|, \lambda), \quad (3)$$

where  $\boldsymbol{\mu} = (\mu_1, \dots, \mu_n)^T$ , and  $p(\cdot, \lambda)$  is a concave penalty function with a tuning parameter  $\lambda \geq 0$ .

For a given  $\lambda > 0$ , define

$$(\hat{\boldsymbol{\mu}}(\lambda), \hat{\boldsymbol{\beta}}(\lambda)) = \operatorname{argmin}_{\boldsymbol{\mu}, \boldsymbol{\beta}} Q_n(\boldsymbol{\mu}, \boldsymbol{\beta}; \lambda).$$

The penalty shrinks some of the pairs  $\mu_j - \mu_k$  to zero. Based on this, we can partition the sample into subgroups. Specifically, let  $\hat{\lambda}$  be the value of the tuning parameter selected based on a data-driven procedure such as the BIC. For simplicity, write  $(\hat{\boldsymbol{\mu}}, \hat{\boldsymbol{\beta}}) \equiv (\hat{\boldsymbol{\mu}}(\hat{\lambda}), \hat{\boldsymbol{\beta}}(\hat{\lambda}))$ . Let  $\{\hat{\alpha}_1, \dots, \hat{\alpha}_{\hat{K}}\}$  be the distinct values of  $\hat{\boldsymbol{\mu}}$ . Let  $\hat{\mathcal{G}}_k = \{i : \hat{\mu}_i = \hat{\alpha}_k, 1 \leq i \leq n\}, 1 \leq k \leq \hat{K}$ . Then  $\{\hat{\mathcal{G}}_1, \dots, \hat{\mathcal{G}}_{\hat{K}}\}$  constitutes a partition of  $\{1, \dots, n\}$ .

An important question is which penalty function should be used here. The  $L_1$  penalty with  $p_\gamma(t, \lambda) = \lambda t$  applies the same thresholding to all pairs  $|\mu_i - \mu_j|$ . As a result, it leads to biased estimates and may not be able to correctly recover the subgroups. This is similar to the situation in variable selection where the lasso tends to over-shrink large coefficients. In

our numerical studies, we found that the  $L_1$  penalty tends to either yield a large number of subgroups or no subgroup on the solution path. Hence, a penalty which can produce unbiased estimates is more appealing. This motivates us to use the concave penalties including the smoothly clipped absolute deviation penalty (SCAD, Fan and Li (2001)) and the minimax concave penalty (MCP, Zhang (2010)). These penalties are asymptotically unbiased and are more aggressive in enforcing a sparser solution. Thus, they are better suited for the current problem, since the number of subgroups is usually much smaller than the sample size.

The MCP has the form

$$p_\gamma(t, \lambda) = \lambda \int_0^t (1 - x/(\gamma\lambda))_+ dx, \gamma > 1,$$

and the SCAD penalty is

$$p_\gamma(t, \lambda) = \lambda \int_0^t \min\{1, (\gamma - x/\lambda)_+ / (\gamma - 1)\} dx, \gamma > 2,$$

where  $\gamma$  is a parameter that controls the concavity of the penalty functions. In particular, both penalties converge to the  $L_1$  penalty as  $\gamma \rightarrow \infty$ . Here and in the rest of the paper, we put  $\gamma$  in the subscript to indicate the dependence of these penalty functions on it. Following Fan and Li (2001) and Zhang (2010), we treat  $\gamma$  as a fixed constant. These concave penalties enjoy the sparsity as the  $L_1$  penalty that it can automatically yield zero estimates. More importantly, it has the unbiasedness property in that it does not shrink large estimated parameters, so that they remain unbiased in the iterations. This property is particularly essential in the ADMM algorithms since the biases in the iterations may significantly affect the search for subgroups.

### 3 Computation

It is difficult to compute the estimates directly by minimizing the objective function (3) due to the fact that the penalty function is not separable in  $\mu_i$ 's. We reparameterize the criterion by introducing a new set of parameters  $\eta_{ij} = \mu_i - \mu_j$ . Then the minimization of

(3) is equivalent to the constraint optimization problem,

$$S(\boldsymbol{\mu}, \boldsymbol{\beta}, \boldsymbol{\eta}) = \frac{1}{2} \sum_{i=1}^n (y_i - \mu_i - \mathbf{x}_i^T \boldsymbol{\beta})^2 + \sum_{i < j} p_\gamma(|\eta_{ij}|, \lambda),$$

$$\text{subject to } \mu_i - \mu_j - \eta_{ij} = 0, \quad (4)$$

where  $\boldsymbol{\eta} = \{\eta_{ij}, i < j\}$ . By the augmented Lagrangian method (ALM), the estimates of the parameters can be obtained by minimizing

$$L(\boldsymbol{\mu}, \boldsymbol{\beta}, \boldsymbol{\eta}, \mathbf{v}) = S(\boldsymbol{\mu}, \boldsymbol{\beta}, \boldsymbol{\eta}) + \sum_{i < j} v_{ij}(\mu_i - \mu_j - \eta_{ij}) + \frac{\vartheta}{2} \sum_{i < j} (\mu_i - \mu_j - \eta_{ij})^2, \quad (5)$$

where the dual variables  $\mathbf{v} = \{v_{ij}, i < j\}$  are Lagrange multipliers and  $\vartheta$  is the penalty parameter. We compute the estimators of  $(\boldsymbol{\mu}, \boldsymbol{\beta}, \boldsymbol{\eta}, \mathbf{v})$  through iterations by the ADMM.

It is noteworthy that by using the concave penalties, although the objective function  $L(\boldsymbol{\mu}, \boldsymbol{\beta}, \boldsymbol{\eta}, \mathbf{v})$  is not a convex function, it is convex with respect to each  $\eta_{ij}$  when  $\gamma > 1/\vartheta$  for the MCP penalty and  $\gamma > 1/\vartheta + 1$  for the SCAD penalty. Moreover, for given  $(\boldsymbol{\mu}, \boldsymbol{\beta}, \boldsymbol{\eta}, \mathbf{v})$ , the minimizer of  $L(\boldsymbol{\mu}, \boldsymbol{\beta}, \boldsymbol{\eta}, \mathbf{v})$  with respect to  $\eta_{ij}$  is unique and has a closed-form expression for the  $L_1$ , MCP and SCAD penalties, respectively. Specifically, for given  $(\boldsymbol{\mu}, \boldsymbol{\beta}, \boldsymbol{\eta}, \mathbf{v})$ , the minimization problem is the same as minimizing

$$\frac{\vartheta}{2}(\delta_{ij} - \eta_{ij})^2 + p_\gamma(|\eta_{ij}|, \lambda) \quad (6)$$

with respect to  $\eta_{ij}$ , where  $\delta_{ij} = \mu_i - \mu_j + \vartheta^{-1}v_{ij}$ . Hence, the closed-form solution for the  $L_1$  penalty is

$$\widehat{\eta}_{ij} = \text{ST}(\delta_{ij}, \lambda/\vartheta), \quad (7)$$

where  $\text{ST}(t, \lambda) = \text{sign}(t)(|t| - \lambda)_+$  is the soft thresholding rule, and  $(x)_+ = x$  if  $x > 0$ , and  $(x)_+ = 0$  otherwise. For the MCP penalty with  $\gamma > 1/\vartheta$ , it is

$$\widehat{\eta}_{ij} = \begin{cases} \frac{\text{ST}(\delta_{ij}, \lambda/\vartheta)}{1 - 1/(\gamma\vartheta)} & \text{if } |\delta_{ij}| \leq \gamma\lambda \\ \delta_{ij} & \text{if } |\delta_{ij}| > \gamma\lambda \end{cases}. \quad (8)$$

For the SCAD penalty with  $\gamma > 1/\vartheta + 1$ , it is

$$\widehat{\eta}_{ij} = \begin{cases} \text{ST}(\delta_{ij}, \lambda/\vartheta) & \text{if } |\delta_{ij}| \leq \lambda + \lambda/\vartheta \\ \frac{\text{ST}(\delta_{ij}, \gamma\lambda/((\gamma-1)\vartheta))}{1 - 1/((\gamma-1)\vartheta)} & \text{if } \lambda + \lambda/\vartheta < |\delta_{ij}| \leq \gamma\lambda \\ \delta_{ij} & \text{if } |\delta_{ij}| > \gamma\lambda \end{cases}. \quad (9)$$

### 3.1 Algorithm

We now describe the computational algorithm based on the ADMM for minimizing the objective function (3). It consists of steps for iteratively updating  $\boldsymbol{\mu}, \boldsymbol{\beta}, \boldsymbol{\eta}$  and  $\mathbf{v}$ . Denote the  $L_2$  norm of any vector  $\mathbf{a}$  by  $\|\mathbf{a}\|$ . The main ingredients of the algorithm are as follows.

First, for a given  $(\boldsymbol{\eta}, \mathbf{v})$ , to obtain an update of  $\boldsymbol{\mu}$  and  $\boldsymbol{\beta}$ , we set the derivatives  $\partial L(\boldsymbol{\mu}, \boldsymbol{\beta}, \boldsymbol{\eta}, \mathbf{v})/\partial \boldsymbol{\mu}$  and  $\partial L(\boldsymbol{\mu}, \boldsymbol{\beta}, \boldsymbol{\eta}, \mathbf{v})/\partial \boldsymbol{\beta}$  to zero, where

$$\begin{aligned} L(\boldsymbol{\mu}, \boldsymbol{\beta}, \boldsymbol{\eta}, \mathbf{v}) &= \frac{1}{2} \sum_{i=1}^n (y_i - \mu_i - \mathbf{x}_i^T \boldsymbol{\beta})^2 + \frac{\vartheta}{2} \sum_{i < j} \{(e_i - e_j)^T \boldsymbol{\mu} - \eta_{ij} + \vartheta^{-1} v_{ij}\}^2 + C \\ &= \frac{1}{2} \|\boldsymbol{\mu} - \mathbf{y} + \mathbf{X}\boldsymbol{\beta}\|^2 + \frac{\vartheta}{2} \|\boldsymbol{\Delta}\boldsymbol{\mu} - \boldsymbol{\eta} + \vartheta^{-1} \mathbf{v}\|^2 + C. \end{aligned} \quad (10)$$

Here  $C$  is a constant independent of  $\boldsymbol{\mu}$  and  $\boldsymbol{\beta}$ ,  $\mathbf{y} = (y_1, \dots, y_n)^T$ ,  $\mathbf{X} = (\mathbf{x}_1, \dots, \mathbf{x}_n)^T$ ,  $e_i$  is the  $i$ th unit  $n \times 1$  vector whose  $i$ th element is 1 and the remaining ones are 0, and  $\boldsymbol{\Delta} = \{(e_i - e_j), i < j\}^T$ . Thus, for given  $\boldsymbol{\eta}^{(m)}$  and  $\mathbf{v}^{(m)}$  at the  $m$ th step, the updates  $\boldsymbol{\mu}^{(m+1)}$  and  $\boldsymbol{\beta}^{(m+1)}$ , which are the minimizers of  $L(\boldsymbol{\mu}, \boldsymbol{\beta}, \boldsymbol{\eta}^{(m)}, \mathbf{v}^{(m)})$ , are

$$\boldsymbol{\mu}^{(m+1)} = (\mathbf{I} + \vartheta \boldsymbol{\Delta}^T \boldsymbol{\Delta} - \mathbf{Q}_{\mathbf{X}})^{-1} \{(\mathbf{I} - \mathbf{Q}_{\mathbf{X}})\mathbf{y} + \vartheta \boldsymbol{\Delta}^T (\boldsymbol{\eta}^{(m)} - \vartheta^{-1} \mathbf{v}^{(m)})\},$$

where  $\mathbf{Q}_{\mathbf{X}} = \mathbf{X}(\mathbf{X}^T \mathbf{X})^{-1} \mathbf{X}^T$ , and

$$\boldsymbol{\beta}^{(m+1)} = (\mathbf{X}^T \mathbf{X})^{-1} \mathbf{X}^T (\mathbf{y} - \boldsymbol{\mu}^{(m+1)}).$$

We further can derive  $\mathbf{I} + \vartheta \boldsymbol{\Delta}^T \boldsymbol{\Delta} = (1 + n\vartheta)\mathbf{I} - \vartheta \mathbf{1}\mathbf{1}^T$ .

Second, the update of  $\eta_{ij}$  at the  $(m+1)$ th iteration is obtained by the formula given in (7), (8) and (9), respectively, by the Lasso, MCP and SCAD penalties with  $\delta_{ij}$  replaced by  $\delta_{ij}^{(m+1)} = \mu_i^{(m+1)} - \mu_j^{(m+1)} + \vartheta^{-1} v_{ij}^{(m)}$ .

Finally, the estimate of  $v_{ij}$  is updated as

$$v_{ij}^{(m+1)} = v_{ij}^{(m)} + \vartheta (\mu_i^{(m+1)} - \mu_j^{(m+1)} - \eta_{ij}^{(m+1)}).$$

Based on the above discussion, the algorithm consists of the following steps:

Step 1. Find initial estimates  $\boldsymbol{\beta}^{(0)}$  from least squares regression by letting  $\mu_i = \mu$  for all  $i$ . Let the initial estimates  $\boldsymbol{\mu}^{(0)} = \mathbf{y} - \mathbf{X}\boldsymbol{\beta}^{(0)}$ ,  $\eta_{ij}^{(0)} = \mu_i^{(0)} - \mu_j^{(0)}$  and  $\mathbf{v}^{(0)} = \mathbf{0}$ .

Step 2. At iteration  $m+1$ , compute  $(\boldsymbol{\mu}^{(m+1)}, \boldsymbol{\beta}^{(m+1)}, \boldsymbol{\eta}^{(m+1)}, \mathbf{v}^{(m+1)})$  by the methods described above.



Step 3. Terminate the algorithm if the stopping rule is met at step  $m + 1$ . Then  $(\boldsymbol{\mu}^{(m+1)}, \boldsymbol{\beta}^{(m+1)}, \boldsymbol{\eta}^{(m+1)}, \boldsymbol{v}^{(m+1)})$  are our final estimates  $(\widehat{\boldsymbol{\mu}}, \widehat{\boldsymbol{\beta}}, \widehat{\boldsymbol{\eta}}, \widehat{\boldsymbol{v}})$ . Otherwise, we go to Step 2.

**Remark 1.** We track the progress of the ADMM based on the primal residual  $\mathbf{r}^{(m+1)} = \Delta\boldsymbol{\mu}^{(m+1)} - \boldsymbol{\eta}^{(m+1)}$ . We stop the algorithm when  $\mathbf{r}^{(m+1)}$  is close to zero such that  $\|\mathbf{r}^{(m+1)}\| < \epsilon$  for some small value  $\epsilon$ .

**Remark 2.** This algorithm enables us to have  $\widehat{\eta}_{ij} = 0$  for a large  $\lambda$ . We put  $y_i$  and  $y_j$  in the same group if  $\widehat{\eta}_{ij} = 0$ . As a result, we have  $\widehat{K}$  estimated groups  $\widehat{\mathcal{G}}_1, \dots, \widehat{\mathcal{G}}_{\widehat{K}}$  and let the estimated intercept for the  $k^{\text{th}}$  group be  $\widehat{\alpha}_k = |\widehat{\mathcal{G}}_k|^{-1} \sum_{i \in \widehat{\mathcal{G}}_k} \widehat{\mu}_i$ , where  $|\widehat{\mathcal{G}}_k|$  is the cardinality of  $\widehat{\mathcal{G}}_k$ .

## 3.2 Convergence of the algorithm

We next consider the convergence properties of the ADMM algorithm.

**Proposition 1.** *The primal residual  $\mathbf{r}^{(m)} = \Delta\boldsymbol{\mu}^{(m)} - \boldsymbol{\eta}^{(m)}$  and the dual residual  $\mathbf{s}^{(m+1)} = \vartheta \Delta^T(\boldsymbol{\eta}^{(m+1)} - \boldsymbol{\eta}^{(m)})$  of the ADMM satisfy that  $\lim_{m \rightarrow \infty} \|\mathbf{r}^{(m)}\|^2 = 0$  and  $\lim_{m \rightarrow \infty} \|\mathbf{s}^{(m)}\|^2 = 0$  for both of the MCP and SCAD penalties.*

The proof of this result is given in the online supplement. Proposition 1 shows that the primal feasibility and dual feasibility are achieved by the algorithm. Therefore, it converges to an optimal point. This optimal point may be a local minimum of the objective function when a concave penalty function is applied.

## 4 Theoretical properties

In this section, we study the theoretical properties of the proposed estimator based on concave penalty functions. Specifically, we derive the order requirement of the minimum difference of signals between groups in order to recover the true groups and the oracle property that under some regularity conditions the oracle estimator is a local minimizer of the objective function with a high probability. Let  $\mathcal{M}_{\mathcal{G}}$  be the subspace of  $R^n$ , defined as

$$\mathcal{M}_{\mathcal{G}} = \{\boldsymbol{\mu} \in R^n : \mu_i = \mu_j, \text{ for any } i, j \in \mathcal{G}_k, 1 \leq k \leq K\}.$$

For each  $\boldsymbol{\mu} \in \mathcal{M}_{\mathcal{G}}$ , it can be written as  $\boldsymbol{\mu} = \mathbf{Z}\boldsymbol{\alpha}$ , where  $\mathbf{Z} = \{z_{ik}\}$  is the  $n \times K$  matrix with  $z_{ik} = 1$  for  $i \in \mathcal{G}_k$  and  $z_{ik} = 0$  otherwise, and  $\boldsymbol{\alpha}$  is a  $K \times 1$  vector of parameters. By matrix calculation, we have  $\mathbf{D} = \mathbf{Z}^T \mathbf{Z} = \text{diag}(|\mathcal{G}_1|, \dots, |\mathcal{G}_K|)$ , where  $|\mathcal{G}_k|$  denotes the number of elements in  $\mathcal{G}_k$ . Define  $|\mathcal{G}_{\min}| = \min_{1 \leq k \leq K} |\mathcal{G}_k|$  and  $|\mathcal{G}_{\max}| = \max_{1 \leq k \leq K} |\mathcal{G}_k|$ . Let  $\mathbf{X} = (\mathbf{X}_1, \dots, \mathbf{X}_p)$ , where  $\mathbf{X}_j$  is the  $j$ th column of  $\mathbf{X}$ . Denote

$$\rho(t) = \lambda^{-1} p_{\gamma}(t, \lambda) \quad \text{and} \quad \bar{\rho}(t) = \rho'(|t|) \text{sgn}(t).$$

For any vector  $\boldsymbol{\zeta} = (\zeta_1, \dots, \zeta_s)^T \in R^s$ , denote  $\|\boldsymbol{\zeta}\|_{\infty} = \max_{1 \leq l \leq s} |\zeta_l|$ . For any symmetric matrix  $\mathbf{A}_{s \times s}$ , denote its  $L_2$  norm as  $\|\mathbf{A}\| = \max_{\boldsymbol{\zeta} \in R^s, \|\boldsymbol{\zeta}\|=1} \|\mathbf{A}\boldsymbol{\zeta}\|$ , and let  $\lambda_{\min}(\mathbf{A})$  and  $\lambda_{\max}(\mathbf{A})$  be the smallest and largest eigenvalues of  $\mathbf{A}$ , respectively. For any matrix  $\mathbf{A} = (A_{ij})_{i=1, j=1}^{s, t}$ , denote  $\|\mathbf{A}\|_{\infty} = \max_{1 \leq i \leq s} \sum_{j=1}^t |A_{ij}|$ . We introduce the following conditions.

- (C1) Assume  $\|\mathbf{X}_j\| = \sqrt{n}$ , for  $1 \leq j \leq p$ ,  $\lambda_{\min}[(\mathbf{Z}, \mathbf{X})^T (\mathbf{Z}, \mathbf{X})] \geq C_1 |\mathcal{G}_{\min}|$ , and  $\|\mathbf{X}\|_{\infty} \leq C_2 p$  for some constants  $0 < C_1 < \infty$  and  $0 < C_2 < \infty$ .
- (C2)  $p_{\gamma}(t, \lambda)$  is a symmetric function of  $t$ , and it is non-decreasing and concave in  $t$  for  $t \in [0, \infty)$ .  $\rho(t)$  is a constant for all  $t \geq a\lambda$  for some constant  $a > 0$ , and  $\rho(0) = 0$ .  $\rho'(t)$  exists and is continuous except for a finite number of  $t$  and  $\rho'(0+) = 1$ .
- (C3) The noise vector  $\boldsymbol{\epsilon} = (\epsilon_1, \dots, \epsilon_n)^T$  has sub-Gaussian tails such that  $P(|\mathbf{a}^T \boldsymbol{\epsilon}| > \|\mathbf{a}\|x) \leq 2 \exp(-c_1 x^2)$  for any vector  $\mathbf{a} \in R^n$  and  $x > 0$ , where  $0 < c_1 < \infty$ .

Conditions (C2) and (C3) are common assumptions in high-dimensional settings. The concave penalties such as MCP and SCAD satisfy Condition (C2). In the literature, it is commonly assumed that the smallest eigenvalue of the design matrix is bounded by  $C_1 n$ , which may not hold for  $(\mathbf{Z}, \mathbf{X})^T (\mathbf{Z}, \mathbf{X})$ . For instance, by letting  $\mathbf{Z}^T \mathbf{X} = \mathbf{0}$  and assuming  $\lambda_{\min}(\mathbf{X}^T \mathbf{X}) = Cn$ , we have

$$\lambda_{\min}[(\mathbf{Z}, \mathbf{X})^T (\mathbf{Z}, \mathbf{X})] \geq \min\{\lambda_{\min}(\mathbf{D}), \lambda_{\min}(\mathbf{X}^T \mathbf{X})\} = \min(|\mathcal{G}_{\min}|, Cn),$$

and  $|\mathcal{G}_{\min}| \leq n/K$ . Therefore, we let the smallest eigenvalue in Condition (C1) be bounded by  $C_1 |\mathcal{G}_{\min}|$ .

When the true group memberships  $\mathcal{G}_1, \dots, \mathcal{G}_K$  are known, the oracle estimators for  $\boldsymbol{\mu}$  and  $\boldsymbol{\beta}$  are

$$(\widehat{\boldsymbol{\mu}}^{or}, \widehat{\boldsymbol{\beta}}^{or}) = \arg \min_{\boldsymbol{\mu} \in \mathcal{M}_{\mathcal{G}}, \boldsymbol{\beta} \in \mathbb{R}^p} \frac{1}{2} \|\mathbf{y} - \boldsymbol{\mu} - \mathbf{X}\boldsymbol{\beta}\|^2, \quad (11)$$

and correspondingly, the oracle estimators for the common intercepts  $\boldsymbol{\alpha}$  and the coefficients  $\boldsymbol{\beta}$  are given by

$$\begin{aligned} (\widehat{\boldsymbol{\alpha}}^{or}, \widehat{\boldsymbol{\beta}}^{or}) &= \arg \min_{\boldsymbol{\alpha} \in \mathbb{R}^K, \boldsymbol{\beta} \in \mathbb{R}^p} \frac{1}{2} \|\mathbf{y} - \mathbf{Z}\boldsymbol{\alpha} - \mathbf{X}\boldsymbol{\beta}\|^2 \\ &= [(\mathbf{Z}, \mathbf{X})^T (\mathbf{Z}, \mathbf{X})]^{-1} (\mathbf{Z}, \mathbf{X})^T \mathbf{y}. \end{aligned}$$

Let  $\boldsymbol{\alpha}^0 = (\alpha_k^0, k = 1, \dots, K)^T$ , where  $\alpha_k^0$  is the underlying common intercept for group  $\mathcal{G}_k$ . Let  $\boldsymbol{\beta}^0$  be the underlying regression coefficient.

**Theorem 1.** *Suppose conditions (C1)-(C3) hold. If  $K = o(n)$ ,  $p = o(n)$ , and*

$$|\mathcal{G}_{\min}| \gg \sqrt{(K+p)n \log n},$$

*we have with probability at least  $1 - 2(K+p)n^{-1}$ ,*

$$\left\| ((\widehat{\boldsymbol{\mu}}^{or} - \boldsymbol{\mu}^0)^T, (\widehat{\boldsymbol{\beta}}^{or} - \boldsymbol{\beta}^0)^T)^T \right\|_{\infty} \leq \phi_n, \quad (12)$$

where

$$\phi_n = c_1^{-1/2} C_1^{-1} \sqrt{K+p} |\mathcal{G}_{\min}|^{-1} \sqrt{n \log n}. \quad (13)$$

Moreover, for any vector  $\mathbf{a}_n \in \mathbb{R}^{K+p}$ , we have as  $n \rightarrow \infty$ ,

$$\sigma_n^{-1}(\mathbf{a}_n) \mathbf{a}_n^T ((\widehat{\boldsymbol{\alpha}}^{or} - \boldsymbol{\alpha}^0)^T, (\widehat{\boldsymbol{\beta}}^{or} - \boldsymbol{\beta}^0)^T)^T \rightarrow N(0, 1), \quad (14)$$

where

$$\sigma_n(\mathbf{a}_n) = \sigma \left\{ \mathbf{a}_n^T [(\mathbf{Z}, \mathbf{X})^T (\mathbf{Z}, \mathbf{X})]^{-1} \mathbf{a}_n \right\}^{1/2}. \quad (15)$$

The proof of this theorem is given in the online supplement.

**Remark 3.** Since  $|\mathcal{G}_{\min}| \leq n/K$ , by the condition  $|\mathcal{G}_{\min}| \gg \sqrt{(K+p)n \log n}$ ,  $K$  and  $p$  must satisfy  $K \sqrt{(K+p)} = o(\sqrt{n(\log n)^{-1}})$ , and hence  $K = o(n^{1/3}(\log n)^{-1/3})$ . By letting  $|\mathcal{G}_{\min}| = \delta n/K$  for some constant  $0 < \delta \leq 1$ , the bound (12) is  $c_1^{-1/2} C_1^{-1} \delta^{-1} K \sqrt{K+p} \sqrt{\log n/n}$ . Moreover, when  $K$  and  $p$  are fixed numbers, the bound (12) is  $C^* \sqrt{\log n/n}$  for some constant  $0 < C^* < \infty$ .

Let

$$b_n = \min_{i \in \mathcal{G}_k, j \in \mathcal{G}_{k'}, k \neq k'} |\mu_i^0 - \mu_j^0| = \min_{k \neq k'} |\alpha_k^0 - \alpha_{k'}^0|$$

be the minimal difference of the common values between two groups.

**Theorem 2.** *Suppose the conditions in Theorem 1 hold. If  $b_n > a\lambda$  and  $\lambda \gg \phi_n$ , where  $\phi_n$  is given in (13), then there exists a local minimizer  $(\widehat{\boldsymbol{\mu}}(\lambda)^T, \widehat{\boldsymbol{\beta}}(\lambda)^T)^T$  of the objective function  $Q_n(\boldsymbol{\mu}, \boldsymbol{\beta}; \lambda)$  given in (3) satisfying*

$$P \left( (\widehat{\boldsymbol{\mu}}(\lambda)^T, \widehat{\boldsymbol{\beta}}(\lambda)^T)^T = ((\widehat{\boldsymbol{\mu}}^{or})^T, (\widehat{\boldsymbol{\beta}}^{or})^T)^T \right) \rightarrow 1.$$

The proof of this theorem is given in the online supplement.

**Remark 4.** The above result holds given that  $b_n \gg \phi_n$ . As discussed in Remark 3, when  $K$  is a finite and fixed number and  $|\mathcal{G}_{\min}| = \delta n/K$  for some constant  $0 < \delta \leq 1$ ,  $b_n \gg C^* \sqrt{\log n/n}$  for some constant  $0 < C^* < \infty$ . Moreover, Theorem 2 shows that the oracle estimator  $((\widehat{\boldsymbol{\mu}}^{or})^T, (\widehat{\boldsymbol{\beta}}^{or})^T)^T$  is a local minimizer  $(\widehat{\boldsymbol{\mu}}(\lambda)^T, \widehat{\boldsymbol{\beta}}(\lambda)^T)^T$  of the objective function with probability approaching 1. Let  $\widehat{\boldsymbol{\alpha}}(\lambda)$  be the distinct values of  $\widehat{\boldsymbol{\mu}}(\lambda)$ . Also  $\widehat{\boldsymbol{\alpha}}^{or}$  consists of the distinct values of  $\widehat{\boldsymbol{\mu}}^{or}$ . By the oracle property in Theorem 2, we have  $P\{\widehat{\boldsymbol{\alpha}}(\lambda) = \widehat{\boldsymbol{\alpha}}^{or}\} \rightarrow 1$ . This result together with the asymptotic normality given in Theorem 1 directly leads to the asymptotic distribution of  $(\widehat{\boldsymbol{\alpha}}(\lambda)^T, \widehat{\boldsymbol{\beta}}(\lambda)^T)^T$  presented in the following corollary.

**Corollary 1.** *Under the conditions in Theorem 2, we have for any vector  $\mathbf{a}_n \in R^{K+p}$ , as  $n \rightarrow \infty$ ,*

$$\sigma_n^{-1}(\mathbf{a}_n) \mathbf{a}_n^T ((\widehat{\boldsymbol{\alpha}}(\lambda) - \boldsymbol{\alpha}^0)^T, (\widehat{\boldsymbol{\beta}}(\lambda) - \boldsymbol{\beta}^0)^T)^T \rightarrow N(0, 1),$$

with  $\sigma_n(\mathbf{a}_n)$  given in (15). As a result, we have for any vectors  $\mathbf{a}_{n1} \in R^K$  and  $\mathbf{a}_{n2} \in R^p$ , as  $n \rightarrow \infty$ ,  $\sigma_{n1}^{-1}(\mathbf{a}_{n1}) \mathbf{a}_{n1}^T (\widehat{\boldsymbol{\alpha}}(\lambda) - \boldsymbol{\alpha}^0) \rightarrow N(0, 1)$  and  $\sigma_{n2}^{-1}(\mathbf{a}_{n2}) \mathbf{a}_{n2}^T (\widehat{\boldsymbol{\beta}}(\lambda) - \boldsymbol{\beta}^0) \rightarrow N(0, 1)$ , where

$$\begin{aligned} \sigma_{n1}(\mathbf{a}_{n1}) &= \sigma \left[ \mathbf{a}_{n1}^T \{ \mathbf{Z}^T \mathbf{Z} - (\mathbf{Z}^T \mathbf{X})(\mathbf{X}^T \mathbf{X})^{-1}(\mathbf{X}^T \mathbf{Z}) \}^{-1} \mathbf{a}_{n1} \right]^{1/2}, \\ \sigma_{n2}(\mathbf{a}_{n2}) &= \sigma \left[ \mathbf{a}_{n2}^T \{ \mathbf{X}^T \mathbf{X} - (\mathbf{X}^T \mathbf{Z})(\mathbf{Z}^T \mathbf{Z})^{-1}(\mathbf{Z}^T \mathbf{X}) \}^{-1} \mathbf{a}_{n2} \right]^{1/2}. \end{aligned}$$

**Remark 5.** The asymptotic distribution of the penalized estimators provides a theoretical justification for further conducting statistical inference about subgrouping. By the results

in Corollary 1, for given  $\mathbf{a}_{n1} \in R^K$  and  $\mathbf{a}_{n2} \in R^p$ ,  $100(1 - \alpha)\%$  confidence intervals for  $\mathbf{a}_{n1}^T \boldsymbol{\mu}^0$  and  $\mathbf{a}_{n2}^T \boldsymbol{\beta}^0$  are given as  $\mathbf{a}_{n1}^T \widehat{\boldsymbol{\alpha}}(\lambda) \pm z_{\alpha/2} \widehat{\sigma}_{n1}(\mathbf{a}_{n1})$  and  $\mathbf{a}_{n2}^T \widehat{\boldsymbol{\beta}}(\lambda) \pm z_{\alpha/2} \widehat{\sigma}_{n2}(\mathbf{a}_{n2})$ , respectively, where  $z_{\alpha/2}$  is the  $(1 - \alpha/2)100$  percentile of the standard normal, and  $\widehat{\sigma}_{n1}(\mathbf{a}_{n1})$  and  $\widehat{\sigma}_{n2}(\mathbf{a}_{n2})$  are estimates of  $\sigma_{n1}(\mathbf{a}_{n1})$  and  $\sigma_{n2}(\mathbf{a}_{n2})$  with  $\sigma^2$  estimated by  $\widehat{\sigma}^2 = (n - \widehat{K} - p)^{-1} \sum_{i=1}^n (y_i - \widehat{\mu}_i - \mathbf{x}_i^T \widehat{\boldsymbol{\beta}})^2$ , where  $\widehat{K}$  is the number of distinct values in  $\widehat{\boldsymbol{\mu}}(\lambda)$ .

## 5 Simulation studies

In this section, we conduct simulation experiments to investigate the numerical performance of our proposed estimators.

We use the modified Bayesian Information Criterion (BIC) (Wang et al (2007)) for high-dimensional data settings to select the tuning parameter by minimizing

$$\text{BIC} = \log\left[\sum_{i=1}^n (y_i - \widehat{\mu}_i - \mathbf{x}_i^T \widehat{\boldsymbol{\beta}})^2 / n\right] + C_n \frac{\log n}{n} (\widehat{K} + p), \quad (16)$$

where  $C_n$  is a positive number which can depend on  $n$ . When  $C_n = 1$ , the modified BIC reduces to the traditional BIC (Schwarz (1978)). Wang et al (2009) used  $C_n = \log(\log(d))$  in their simulation study when the number of predictors which is  $d$  diverges with sample size. In this paper, we adopt the same strategy and let  $C_n = c \log(\log(d))$ , where  $d = n + p$  and  $c$  is a positive constant. In our analysis, we select  $\lambda$  by minimizing the modified BIC and use a fixed value for  $\vartheta$  and  $\gamma$ .

**Example 1.** We simulate data from the model

$$y_i = \mu_i + \mathbf{x}_i^T \boldsymbol{\beta} + \epsilon_i, i = 1, \dots, n, \quad (17)$$

where  $\mathbf{x}_i = (x_{i1}, \dots, x_{i5})^T$  are generated from the multivariate normal distribution with mean 0, variance 1 and an exchangeable correlation  $\rho = 0.3$  and the error terms  $\epsilon_i$  are from independent  $N(0, 0.5^2)$ . We simulate  $\boldsymbol{\beta} = (\boldsymbol{\beta}_1, \dots, \boldsymbol{\beta}_5)^T$  from independent Uniform[0.5, 1]. We generate  $\mu_i$  from two different values  $-\alpha$  and  $\alpha$  with equal probabilities, i.e., we generate them from the distribution:  $p(\mu_i = -\alpha) = p(\mu_i = \alpha) = 1/2$ , so that there are two intercepts  $\alpha_1 = -\alpha$  and  $\alpha_2 = \alpha$ . In our simulation studies, we take different values of  $\alpha$  for illustration of our proposed method. It is noteworthy that for smaller value of  $\alpha$ , it is more difficult to identify the two groups.

In our analysis, we choose to fix  $\vartheta = 1$  and  $\gamma = 3$ . We compare the performance of the estimators with the ADMM algorithm by using the two concave penalties (MCP and SCAD) and using a weighted  $L_1$  penalty

$$p_\gamma(|\mu_i - \mu_j|, \lambda) = \lambda \omega_{ij} |\mu_i - \mu_j|,$$

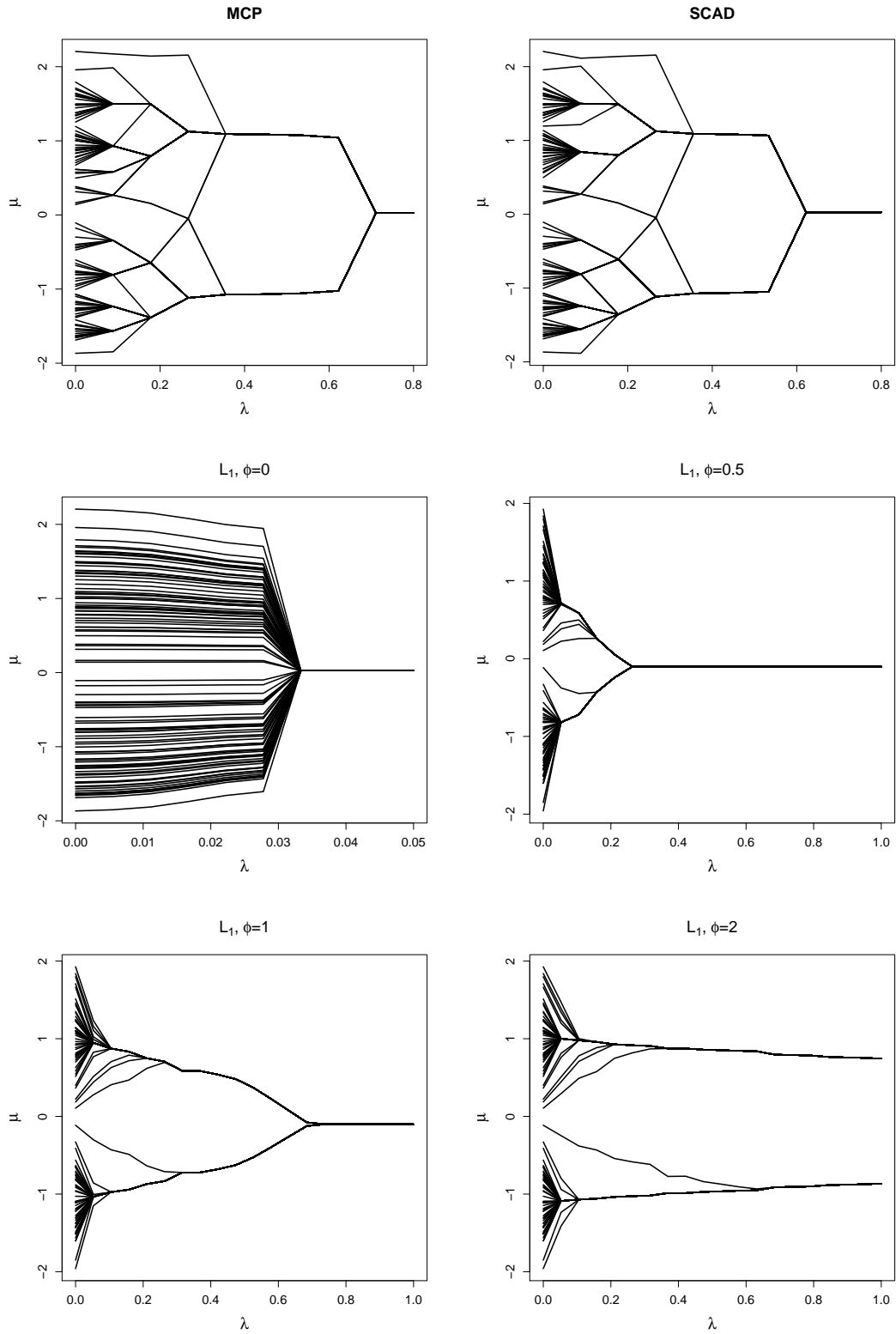
which requires specification of the weights  $\omega_{ij}$ . As discussed in Chi and Lange (2001), the choice of the weights can dramatically affect the quality of the results in cluster analysis. In the regression context such as in our study, it is even more challenging to select the weights.

For the  $L_1$  penalty, we let the weight be  $\omega_{ij} = \exp(-\phi(y_i - y_j)^2)$  which is a Gaussian kernel defined on the distance of two points. The constant  $\phi$  is nonnegative. When  $\phi = 0$ , it corresponds to the Lasso penalty. Note that it is unclear what weights we need to apply to obtain optimal results. We here use the Gaussian kernel as the weight to illustrate this point by using different values for  $\phi$ .

Figure 1 displays the solution paths for the means  $(\mu_1, \dots, \mu_n)$  against  $\lambda$  values by using MCP and SCAD, and the  $L_1$  penalties with  $\phi = 0, 0.5, 1, 2$ , respectively, based on one sample with  $n = 100$  and  $\alpha = 1$ . We observe that the MCP and SCAD have similar solution paths as shown in Figure 1. For these two penalties, the estimated values for  $\boldsymbol{\mu}$  converge to two different values around  $-1$  and  $1$  which are the true values for the intercepts of the two groups, when  $\lambda$  reaches certain value (around 0.38 for both MCP and SCAD). They eventually converge to one value when  $\lambda$  exceeds 0.6. The  $L_1$  penalty, however, shows a different solution path from MCP and SCAD, and the solution paths look quite differently for different values of  $\phi$ , so that the choice of weights can dramatically affect the estimation results. When  $\phi = 0$  which is the LASSO penalty, we see that the estimated values for  $\mu_i$ 's converge quickly as the  $\lambda$  value increases until they converge to a common point around 0 when  $\lambda$  reaches 0.035. As a result, it cannot effectively identify the groups of the  $\boldsymbol{\mu}$  value. By looking at the plots for  $\phi = 0.5, 1, 2$ , we observe that as the  $\phi$  value becomes larger, the estimated values converge to one point more slowly.

Next we conduct the simulations by selecting  $\lambda$  via minimizing the modified BIC given in (16). Recall that we let  $C_n = c \log(\log(n + p))$ , where  $n + p$  is the number of components in  $\boldsymbol{\mu}$  and  $\boldsymbol{\beta}$ , and  $c$  is a positive constant. We use different  $c$  values by letting  $c = 5, 10$

Figure 1: Solution paths for the means  $(\mu_1, \dots, \mu_n)$  against  $\lambda$  values by using MCP, SCAD and  $L_1$  penalties, respectively, in Example 1.



in our estimation procedure. We consider different values for  $\alpha$  by letting  $\alpha = 1, 1.5, 2$ , so that the difference of the true common values between the two groups varies from 2 to 4. Table 1 reports the mean, the median and standard error (s.e.) of the estimated number of groups  $\widehat{K}$  by the MCP, SCAD and  $L_1$  methods with  $\phi = 1$  and 2 based on 100 simulation realizations with  $n = 100$ . Moreover, to study the estimation accuracy, in Table 2 we report the average value and the standard error shown in the parentheses of the square root of the mean squared errors (MSE) for the estimated values of  $\boldsymbol{\mu}$  and  $\boldsymbol{\beta}$  for the MCP, SCAD and  $L_1$  estimators and the oracle estimator given in (11). The square roots of the MSE for  $\boldsymbol{\mu}$  and  $\boldsymbol{\beta}$  are, respectively, defined as  $\|\widehat{\boldsymbol{\mu}} - \boldsymbol{\mu}\|/\sqrt{n}$  and  $\|\widehat{\boldsymbol{\beta}} - \boldsymbol{\beta}\|/\sqrt{p}$  for each realization.

Table 1: The mean, median and standard error (s.e.) of  $\widehat{K}$  by the MCP, SCAD and  $L_1$  methods with  $\phi = 1.0$  and 2.0 based on 100 realizations with  $n = 100$  in Example 1.

$c$	$\alpha$	1.0			1.5			2.0		
		mean	median	s.e.	mean	median	s.e.	mean	median	s.e.
5.0	MCP	2.57	2.00	0.90	2.41	2.00	0.93	2.10	2.00	0.44
	SCAD	2.58	2.00	0.96	2.37	2.00	0.90	2.18	2.00	0.63
	$L_1(\phi = 1.0)$	1.76	1.00	0.99	2.71	3.00	0.88	2.50	2.00	0.82
	$L_1(\phi = 2.0)$	3.03	3.00	1.16	3.13	3.00	1.19	3.25	3.00	1.00
10.0	MCP	2.10	2.00	0.33	2.04	2.00	0.20	2.01	2.00	0.11
	SCAD	2.11	2.00	0.35	2.04	2.00	0.20	2.02	2.00	0.14
	$L_1(\phi = 1.0)$	1.40	1.00	0.65	5.10	4.00	3.00	3.75	3.00	1.60
	$L_1(\phi = 2.0)$	2.29	2.00	0.78	3.03	3.00	1.02	3.25	3.00	1.00

In Table 1, for both MCP and SCAD methods we observe that the median value of  $\widehat{K}$  among the 100 replications is 2 for all cases, which is the true number of groups in our model, and the mean values are close to 2 for different values of  $\alpha$ . For larger value of  $\alpha$ , it is easier to detect the subgroups, so that correspondingly we observe that the mean values of  $\widehat{K}$  are closer to 2 for larger  $\alpha$ . The MCP and SCAD can identify the groups for both values of  $c$ , although they perform better with  $c = 10$  by having smaller standard errors. The



Table 2: The mean and standard error (s.e.) shown in parentheses of the square root of the MSE for the estimated values of  $\boldsymbol{\mu}$  and  $\boldsymbol{\beta}$  for the MCP, SCAD and  $L_1$  penalty estimators and the oracle estimators with  $\phi = 1.0$  and  $2.0$  based on 100 realizations with  $n = 100$  in Example 1.

$c$	$\boldsymbol{\alpha}$	$\boldsymbol{\mu}$			$\boldsymbol{\beta}$		
		1.0	1.5	2.0	1.0	1.5	2.0
5.0	MCP	0.409 (0.108)	0.246 ( 0.192)	0.132 (0.151)	0.043 (0.034)	0.076 (0.045)	0.062 (0.038)
	SCAD	0.414 (0.116)	0.240 (0.190)	0.158 (0.168)	0.091 (0.036)	0.075 (0.044)	0.065 (0.040)
	$L_1(\phi = 1.0)$	0.874 ( 0.202)	0.370 (0.237)	0.185 (0.173)	0.118 (0.040)	0.084 (0.047)	0.066 (0.036)
	$L_1(\phi = 2.0)$	0.637 (0.226)	0.274 (0.180)	0.167 (0.153)	0.106 ( 0.040)	0.076 (0.041)	0.064 (0.035)
10.0	MCP	0.407 (0.139)	0.230 (0.178)	0.154 (0.164)	0.086 (0.035)	0.069 (0.034)	0.062 (0.030)
	SCAD	0.409 (0.138)	0.234 (0.178)	0.155 (0.163)	0.086 (0.034)	0.069 (0.035)	0.061 (0.030)
	$L_1(\phi = 1.0)$	0.946 ( 0.138)	0.265 (0.142)	0.203 (0.169)	0.121 ( 0.039)	0.075 (0.038)	0.069 (0.038)
	$L_1(\phi = 2.0)$	0.769 (0.215)	0.287 (0.210)	0.167 (0.153)	0.113 ( 0.039)	0.078 (0.046)	0.064 ( 0.035)

$L_1$  penalties with both values for  $\phi$  in general have worse performance than the MCP and SCAD penalties. They have mean and median values for  $\widehat{K}$  further away from 2 and larger standard errors. Moreover, the performance of the  $L_1$  penalty is not stable. The  $L_1$  penalty with  $\phi = 1$  tends to select less than two groups for  $\alpha = 1.0$  and more than two groups for  $\alpha = 1.5, 2.0$ , while the  $L_1$  penalty with  $\phi = 2$  tends to select more groups in general. For  $\alpha = 1.5$  and  $2.0$  and  $c = 5.0$ , the  $L_1$  penalty with  $\phi = 1$  performs better than the  $L_1$  penalty with  $\phi = 2$  by having  $\widehat{K}$  values closer to two and smaller standard errors, but for other cases the  $L_1$  penalty with  $\phi = 2$  seems to perform better. Thus, we see that different weights applied to the  $L_1$  penalty may significantly affect the performance of the resulting estimator, and there is no clear rule on what weight to be used in the general situation. Table 2 shows that the MCP and SCAD methods have smaller MSE values than the  $L_1$  penalty methods in general since they have more accurate selection results and produce less biased estimates.

To evaluate the asymptotic normality established in Corollary 1, Table 3 lists the empirical bias (Bias) for the estimates of the two intercepts  $\alpha_1$  and  $\alpha_2$ , and it also presents the average asymptotic standard error (ASE) calculated according to Corollary 1 and the empirical standard error (ESE) based on 100 replications for the MCP and SCAD methods with  $c = 10$  as well as the oracle estimator (ORACLE). The biases are around zero for all cases. Moreover, we observe that the asymptotic standard errors for the MCP and SCAD methods are similar to those for the ORACLE estimator. This result supports our asymptotic normality result in Corollary 1.

Lastly, we conduct inferences on the difference between groups. Table 4 presents the average p-values for testing  $\mathcal{H}_0 : \alpha_1 = \alpha_2$  based on the 100 simulation realizations. We use  $\sigma_{n1}(\mathbf{a})^{-1}(\widehat{\alpha}_1(\lambda) - \widehat{\alpha}_2(\lambda))$ ,  $\mathbf{a} = (1, -1)$ , as the test statistic which has the asymptotic normal distribution given in Corollary 1, and the estimates  $\widehat{\alpha}_1(\lambda)$  and  $\widehat{\alpha}_2(\lambda)$  are obtained by the MCP and SCAD methods with  $c = 10$ . We obtain the p-values close to zero for all cases, so that the difference between the groups is further confirmed by the inference procedure.

**Example 2.** We simulate data from model (17) with the predictors, the error terms and the coefficients  $\beta$  generated from the same distributions as given in Example 1. We simulate  $\mu_i$  from three different values  $-2, 0, 2$  with equal probabilities. We use the modified BIC to select the tuning parameter  $\lambda$  by letting  $C_n = 5 \log(\log(n+p))$ . Figure 2 shows the boxplots

Table 3: The empirical bias (Bias) for the estimates of  $\alpha_1$  and  $\alpha_2$ , and the average asymptotic standard error (ASE) calculated according to Corollary 1 and the empirical standard error (ESE) based on 100 replications for the MCP and SCAD methods and the oracle estimator (ORACLE) with  $c = 10$  in Example 1.

		$\alpha = 1.0$		$\alpha = 1.5$		$\alpha = 2.0$	
		$\alpha_1$	$\alpha_2$	$\alpha_1$	$\alpha_2$	$\alpha_1$	$\alpha_2$
MCP	Bias	0.037	-0.066	0.031	-0.055	0.065	-0.083
	ASE	0.071	0.070	0.072	0.071	0.075	0.074
	ESE	0.104	0.117	0.085	0.092	0.085	0.092
SCAD	Bias	0.040	0.069	0.036	-0.060	0.067	-0.087
	ASE	0.071	0.070	0.072	0.071	0.075	0.074
	ESE	0.103	0.119	0.085	0.094	0.084	0.094
ORACLE	Bias	-0.009	-0.005	-0.010	-0.005	-0.010	-0.005
	ASE	0.072	0.072	0.072	0.072	0.072	0.072
	ESE	0.070	0.067	0.070	0.067	0.070	0.067

Table 4: The average p-values for testing  $\mathcal{H}_0 : \alpha_1 = \alpha_2$  based on the 100 simulation realizations with the estimates  $\hat{\alpha}_1(\lambda)$  and  $\hat{\alpha}_2(\lambda)$  obtained by the MCP and SCAD methods with  $c = 10$  in Example 1.

$\alpha$	1.0	1.5	2.0
MCP	< 0.001	< 0.001	< 0.001
SCAD	< 0.001	< 0.001	< 0.001

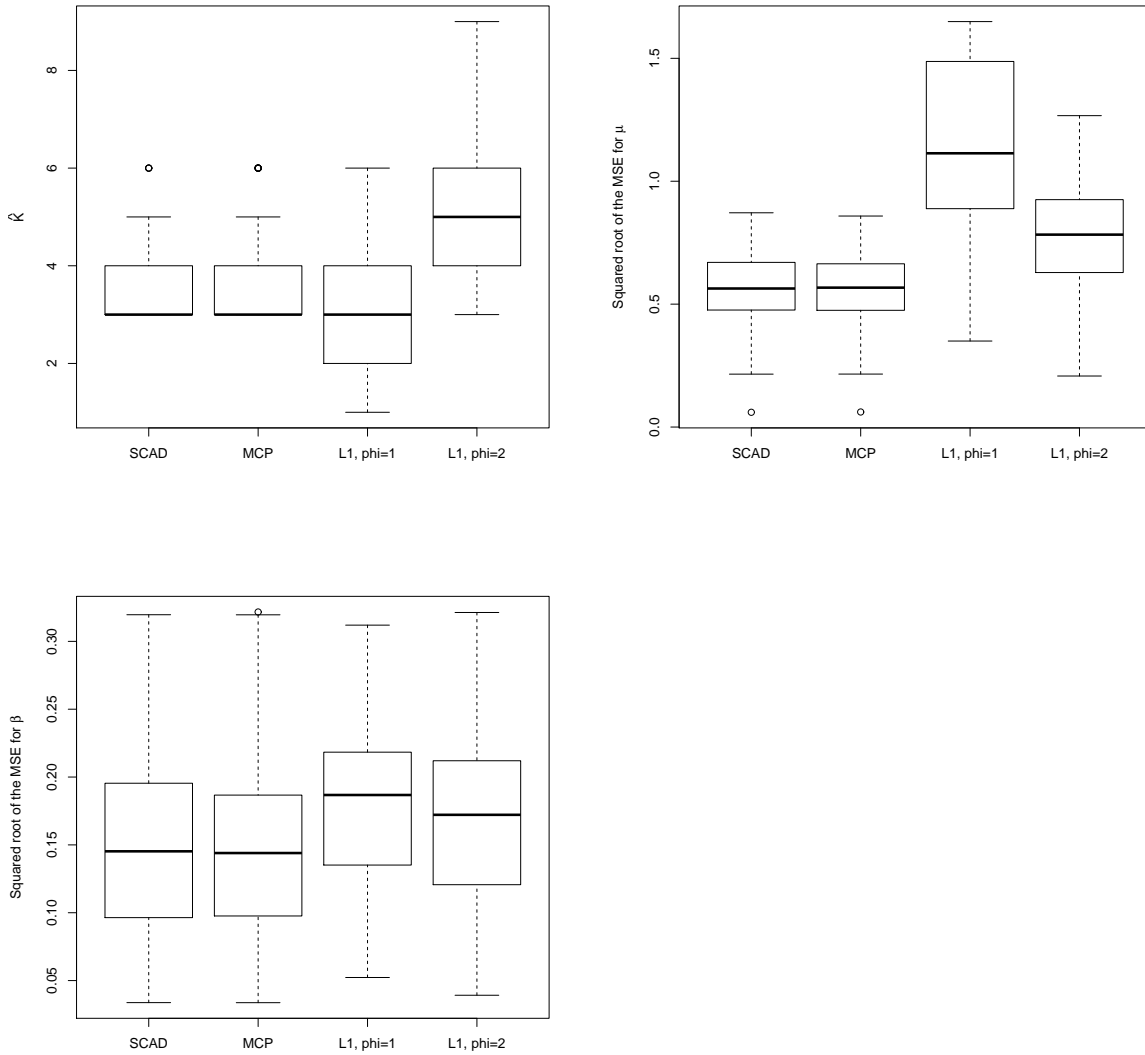
of the estimated number of subgroups  $\widehat{K}$  and the square root of the MSE for the estimated values of  $\boldsymbol{\mu}$  and  $\boldsymbol{\beta}$ , respectively, by using MCP, SCAD and  $L_1$  penalty with  $\phi = 1, 2$  methods based on 100 simulation realization with  $n = 100$ . In the first plot, we observe that for the MCP and SCAD methods, the median value for  $\widehat{K}$  is 3, which is the true number of groups in our model. For some replications, they select more groups than three. For the  $L_1$  penalty with  $\phi = 1$ , the median value for  $\widehat{K}$  is 3 as well. However, some replications have more than three and others have less than three for the  $\widehat{K}$  value. Moreover, for this example, the  $L_1$  penalty with  $\phi = 2$  tends to select more groups in all replications. The other two plots show that the MCP and SCAD have much smaller MSE values than the two  $L_1$  penalty methods.

**Example 3.** We generate data from a homogeneous model given as  $y_i = \mu + \mathbf{x}_i^T \boldsymbol{\beta} + \epsilon_i, i = 1, \dots, 100$ . The predictors, the error term and the coefficients are simulated in the same way as in Example 1. Let  $\mu = 2$ . We fit the heterogeneous model (1) by using our proposed method. In practice, we choose the value of  $\lambda$  by the modified BIC method as illustrated in Examples 1 and 2. In this example, for illustration of our penalization estimation and the subsequent inference method for subgroup identification in the homogeneous model, we use a set of different values for the tuning parameter  $\lambda$ . For small values of  $\lambda$ , we expect to have more identified groups. We further conduct inference on heterogeneity between groups by using the asymptotic normality in Corollary 1.

To test on heterogeneity, we formulate the hypothesis that  $\mathcal{H}_0 : \alpha_1 = (|\widehat{K}| - 1)^{-1} \sum_{j=2}^{|\widehat{K}|} \alpha_j$ , where  $\alpha_1$  is the intercept for the largest group, so that we test on the difference of the intercept for the largest group and the average intercept for other groups. For demonstration of our inference procedure applying to the homogeneous model, we choose a set of small values  $\lambda = (0.15, 0.20, 0.25)$ , so that more than one groups are identified by the penalization procedure. For small values of  $\lambda$ , since subgroups with small sizes may be identified, we adjust to estimate  $\sigma^2$  by  $\widehat{\sigma}^2 = (n - 2 - p)^{-1} \sum_{i=1}^n (y_i - \widehat{\mu}_i - \mathbf{x}_i^T \widehat{\boldsymbol{\beta}})^2$ , where  $\widehat{\mu}_i = \widehat{\alpha}_1$  for  $i \in \mathcal{G}_1$  and  $\widehat{\mu}_i = (|\widehat{K}| - 1)^{-1} \sum_{j=2}^{|\widehat{K}|} \widehat{\alpha}_j$  otherwise. Figure 3 shows the boxplots of the p-values for the hypothesis testing based on the 100 simulation realizations for different values of  $\lambda$ . The estimates of the intercepts are obtained by the MCP and SCAD methods, respectively. We observe that the median values of the p-values are large in general.

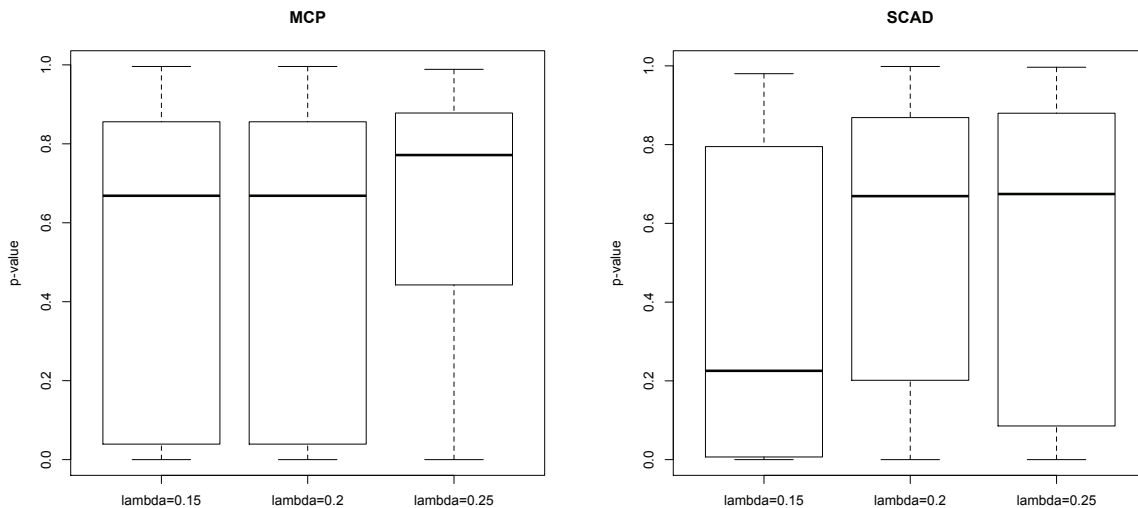
**Example 4. Case 1.** We simulate data from the same data generating process as Exam-

Figure 2: Boxplots of the estimated number of subgroups  $\hat{K}$  and the square root of the MSE for the estimated values of  $\boldsymbol{\mu}$  and  $\boldsymbol{\beta}$ , respectively, by using MCP, SCAD and  $L_1$  with  $\phi = 1, 2$  methods based on 100 simulation realizations with  $n = 100$  in Example 2.



ple 2, so that the data are generated from three groups with the same size (balanced groups). In this example, we aim to compare the performance of cluster analysis by using different penalties including MCP, SCAD, and truncated  $L_1$  as well as by using the Gaussian mixture model-based clustering algorithm from the R package of MCLUST (Fraley and Raftery

Figure 3: Boxplots of the p-values for the hypothesis testing in Example 3 based on the 100 simulation realizations for different values of  $\lambda$ .



(2002)). In our regression setting, we need to apply MCLUST to  $y_i - \mathbf{x}_i^T \boldsymbol{\beta}$  for cluster analysis. One simple way is to obtain the estimate  $\hat{\boldsymbol{\beta}}$  of  $\boldsymbol{\beta}$  by the ordinary least squares (OLS) first, and then apply the MCLUST to the pseudo observations  $y_i - \mathbf{x}_i^T \hat{\boldsymbol{\beta}}$ , which is adopted in our numerical analysis.

For the penalized methods, we apply the same iterative algorithm as described in Section 3.1 to obtain the parameter estimates by using different penalties. The same BIC method is applied to choose the tuning parameter as described in Example 2. It is worth noting that the rest steps remain the same except for the estimation of  $\eta_{ij}$ , which needs some modifications due to the use of different penalties. Specifically, for the truncated  $L_1$  penalty which has the form  $p(|t|, \lambda; \tau) = \lambda \min(|t|; \tau)$ , where  $\tau$  is the thresholding parameter, the estimate of  $\eta_{ij}$  is obtained by minimizing  $h(\eta_{ij}) = \frac{\vartheta}{2}(\delta_{ij} - \eta_{ij})^2 + \lambda \min(|\eta_{ij}|; \tau)$ . We then apply the difference of convex programming technique as given in (Shen and Huang (2010)) to obtain the minimizer of  $h(\eta_{ij})$ . In this algorithm, the function  $h(\eta_{ij})$  needs to be decomposed into difference of two convex functions  $h_1(\eta_{ij}) - h_2(\eta_{ij})$ , where  $h_1(\eta_{ij}) = \frac{\vartheta}{2}(\delta_{ij} - \eta_{ij})^2 + \lambda|\eta_{ij}|$  and  $h_2(\eta_{ij}) = \lambda(|\eta_{ij}| - \tau)_+$ . This enables us to approximate  $h(\eta_{ij})$  by an upper convex function

at iteration  $m + 1$  which results in

$$\widehat{\eta}_{ij}^{(m+1)} = \begin{cases} \widehat{\delta}_{ij}^{(m+1)} & \text{if } |\widehat{\eta}_{ij}^{(m)}| \geq \tau \\ \left( |\widehat{\delta}_{ij}^{(m+1)}| - \lambda/\vartheta \right)_+ \left( \widehat{\delta}_{ij}^{(m+1)} / |\widehat{\delta}_{ij}^{(m+1)}| \right) & \text{otherwise} \end{cases}.$$

One important evaluation criterion for clustering methods is based on their ability to reconstruct the true underlying cluster structure. We, therefore, use the Rand Index measure (Rand (1971)) to evaluate the accuracy of the clustering results. The Rand Index is viewed as a measure of the percentage of correct decisions made by the algorithm. It is computed by using the formula:

$$\text{RI} = \frac{\text{TP} + \text{TN}}{\text{TP} + \text{FP} + \text{FN} + \text{TN}},$$

where a true positive (TP) decision assigns two observations from the same ground truth group to the same cluster, a true negative (TN) decision assigns two observations from different groups to different clusters, a false positive (FP) decision assigns two observations from different groups to the same cluster, and a false negative (FN) decision assigns two observations from the same group to different clusters. The Rand Index lies between 0 and 1. Higher values of the Rand Index indicate better performance of the algorithm.

Table 5 presents the mean and standard error (s.e.) of  $\widehat{K}$ , the square root of the MSE (SMSE) for the estimated  $\boldsymbol{\mu}$  and the clustering accuracy (Accuracy) by different methods. For the truncated  $L_1$ , by taking the same strategy as Shen and Huang (2010), we use different values  $\tau = 0.5, 1.0, 1.5$  for the thresholding parameter. In the MCLUST column, it shows the results by using the MCLUST package with the number of groups selected by the BIC method which is the default method in the MCLUST package and is widely used for determining the number of clusters in practice. In the MCLUST-MCP column, it shows the results by using the MCLUST package with the number of groups determined by our proposed penalized approach with MCP penalty.

From Table 5, we observe that the proposed concave fusion penalized methods, MCP and SCAD, have better performance than other methods. They have higher clustering accuracy rates and smaller SMSE values for  $\widehat{\boldsymbol{\mu}}$  than others. This result is further reflected by the boxplots in Figure 4 of accuracy rates for the MCP, SCAD, truncated  $L_1$  with  $\tau = 1.0$ , and MCLUST methods. For the truncated  $L_1$ , it has the best performance at  $\tau = 1.0$  among

Table 5: The mean and standard error (s.e.) of  $\widehat{K}$  and the square root of the MSE (SMSE) for the estimated  $\boldsymbol{\mu}$  as well as the clustering accuracy (Accuracy) by different methods based on 100 realizations with  $n = 100$  for Case 1 of Example 4 with balanced groups.

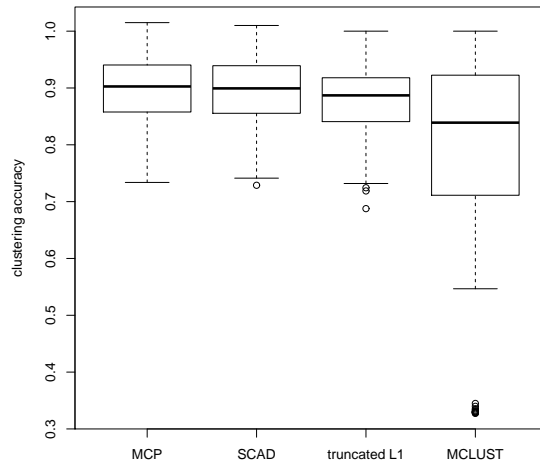
		MCP	SCAD	Truncated $L_1$			MCLUST	MCLUST-MCP
				$\tau = 0.5$	$\tau = 1.0$	$\tau = 1.5$		
$K$	mean	3.570	3.600	6.930	3.960	2.390	2.400	—
	s.e.	0.671	0.696	0.956	0.887	0.737	0.711	—
SMSE of $\boldsymbol{\mu}$	mean	0.589	0.585	0.597	0.605	0.963	0.791	0.607
	s.e.	0.157	0.154	0.158	0.164	0.195	0.380	0.134
Accuracy	mean	0.897	0.892	0.829	0.873	0.707	0.777	0.864
	s.e.	0.059	0.057	0.066	0.064	0.112	0.193	0.058

the three different values for  $\tau$ . Moreover, the three penalized methods, MCP, SCAD and truncated  $L_1$  with  $\tau = 1.0$ , can identify the cluster membership more correctly than the MCLUST method by observing higher accuracy rates. The MCP improves the accuracy rate by 15.4% compared to the MCLUST. It is worth noting that in order to apply the Gaussian mixture model-based method, how many clusters to be used is always crucial. For the MCLUST-MCP, instead of using the BIC, we use our proposed penalized MCP approach to determine the number of clusters and then apply the MCLUST, we see that the accuracy rate is improved compared to the MCLUST with the BIC method. This result indicates that our proposed concave penalized method also provides a possible tool to determine the number of clusters for the Gaussian mixture model-based method.

**Case 2.** In this setting, we generate data from three groups with different sizes (un-balanced groups). We consider two simulation designs: Design 1:  $\mu_i$ 's are generated from three different values  $-2, 0, 2$  with probabilities 0.2, 0.3, 0.5, respectively, and Design 2:  $\mu_i$ 's are generated from  $-2, 0, 2$  with probabilities 0.1, 0.3, 0.6, respectively. Other terms are simulated according to the same setting as Case 1. Table 6 presents the mean and standard error (s.e.) of  $\widehat{K}$ , the square root of the MSE (SMSE) for the estimated  $\boldsymbol{\mu}$  and the cluster-



Figure 4: Boxplots of the clustering accuracy for the MCP, SCAD, truncated  $L_1$  and MCLUST based on the 100 simulation realizations in Case 1 of Example 4.



ing accuracy (Accuracy) by the MCP, SCAD, truncated  $L_1$ , MCLUST and MCLUST-MCP based on 100 realizations. We see that for the MCP, SCAD and truncated  $L_1$  methods, the performance for the two unbalanced designs is comparable to that for the balanced design in Case 1. Again the MCP and SCAD outperform the other methods. The performance of MCLUST-MCP shows improvement over MCLUST. For the MCLUST, the estimated number of groups  $\hat{K}$  decreases as the design becomes more unbalanced. The smallest group is not successfully identified for most replications. For the penalized method, however, the  $\hat{K}$  values remain similar for different designs. Hence, the MCLUST may be more sensitive to cluster sizes based on these simulation results.

## 6 Empirical example

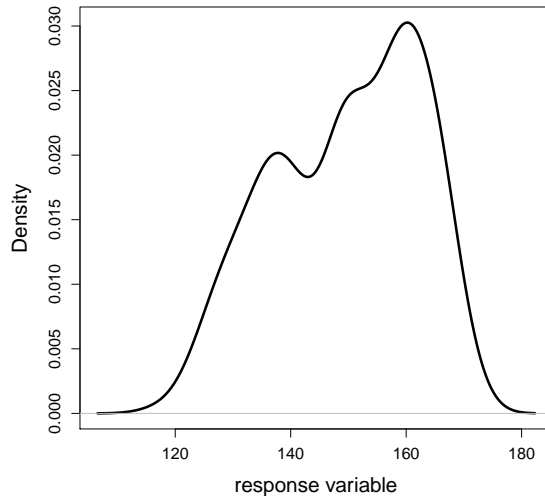
In this section, we use the Cleveland Heart Disease Dataset to illustrate our method. This dataset is available at the UCI machine learning repository. The dataset has 13 clinical measurements on 297 individuals. As described in Lauer et al (1999), the maximum heart rate achieved (thalach) variable is related to cardiac mortality. In addition, some categorical

Table 6: The mean and standard error (s.e.) of  $\widehat{K}$  and the square root of the MSE (SMSE) for the estimated  $\boldsymbol{\mu}$  as well as the clustering accuracy (Accuracy) by different methods based on 100 realizations with  $n = 100$  for Case 2 of Example 4 with unbalanced groups.

		MCP	SCAD	Truncated $L_1$			MCLUST	MCLUST-MCP
				$\tau = 0.5$	$\tau = 1.0$	$\tau = 1.5$		
Design 1								
$K$	mean	3.730	3.660	6.540	3.870	2.360	2.380	—
	s.e.	0.670	0.713	1.049	0.928	0.659	0.663	—
SMSE of $\boldsymbol{\mu}$	mean	0.561	0.556	0.585	0.577	0.893	0.771	0.592
	s.e.	0.126	0.130	0.127	0.146	0.135	0.309	0.124
Accuracy	mean	0.890	0.891	0.822	0.872	0.733	0.792	0.846
	s.e.	0.048	0.048	0.051	0.058	0.092	0.152	0.064
Design 2								
$K$	mean	3.700	3.730	6.350	3.960	2.690	2.230	—
	s.e.	0.717	0.709	0.880	1.197	1.473	0.679	—
SMSE of $\boldsymbol{\mu}$	mean	0.488	0.487	0.522	0.502	0.852	0.763	0.579
	s.e.	0.121	0.120	0.122	0.127	0.135	0.220	0.148
Accuracy	mean	0.898	0.899	0.823	0.877	0.713	0.793	0.818
	s.e.	0.048	0.047	0.056	0.054	0.118	0.123	0.097

variables are also used to check heart problems including chest pain type, exercise induced angina indicator, ST depression induced by exercise relative to rest, slope of the peak exercise ST segment, number of major vessels colored by fluoroscopy and the heart status (normal=3; fixed defect=6; reversible defect=7). We use the fitted value of thalach as the response variable by projecting it onto the linear space spanned by the categorical variables. Our interest is to conduct subgroup analysis for the fitted value of thalach as the response  $y$  after adjusting for the effects of the covariates:  $x_1$  =age in years;  $x_2$  =gender;  $x_3$  =resting blood pressure;  $x_4$  =serum cholesterol;  $x_5$  =fasting blood sugar indicator; and  $x_6$  =resting

Figure 5: Density plot of the response variable after adjusting for the effects of the covariates for the empirical example.



electrocardiographic results.

We first plot the kernel density estimates of  $y_i - \mathbf{x}_i^T \hat{\boldsymbol{\beta}}$  in Figure 5, where  $\hat{\boldsymbol{\beta}}$  is obtained from OLS estimation. Clearly, we see that after adjusting for the effects of the covariates, the distribution in Figure 5 still shows multiple modes. The heterogeneity may be caused by some unobserved latent factors. Hence, it is not suitable to fit a standard linear regression model with a common intercept by using the response and the predictors. Instead we fit the heterogeneous model  $y_i = \mu_i + \mathbf{x}_i^T \boldsymbol{\beta} + \epsilon_i, i = 1, \dots, 297$ , and we identify subgroups by our proposed ADMM algorithm. We select the tuning parameter by minimizing the modified BIC in a certain range by following the same rule as given in Example 2 of Section 5. As a result, two major groups are identified by both of the MCP and SCAD methods. We also conduct inference by testing the difference of the intercepts for the two identified groups by using the asymptotic normality in Corollary 1, and we find that the p-values are close to zero for both of the MCP and SCAD methods.

In Table 7 we report the estimated coefficients  $\hat{\boldsymbol{\beta}}$ , their standard deviations (s.d.) and the p-values for testing the significance of the coefficients by the proposed method with the MCP and SCAD pairwise fusion, and the OLS estimation by assuming a common intercept.

Table 7: The estimated values (est) for the coefficients  $\beta$ , their standard deviations (s.d.) and the p-values for testing the significance of the coefficients by the OLS, MCP and SCAD, respectively.

		$\beta_1$	$\beta_2$	$\beta_3$	$\beta_4$	$\beta_5$	$\beta_6$
OLS	est	-0.345	-4.120	-0.028	-0.008	0.183	-1.359
	s.d.	0.083	1.534	0.042	0.0142	2.031	0.725
	p-value	< 0.001	0.007	0.502	0.563	0.928	0.061
MCP	est	-0.355	-3.825	-0.007	-0.006	0.628	-1.849
	s.d.	0.040	0.752	0.021	0.007	1.016	0.354
	p-value	< 0.001	< 0.001	0.563	0.558	0.283	< 0.001
SCAD	est	-0.358	-3.698	-0.012	-0.004	1.091	-2.129
	s.d.	0.040	0.743	0.021	0.007	1.005	0.351
	p-value	< 0.001	< 0.001	0.558	0.554	0.278	< 0.001

The standard deviation for the MCP and SCAD methods is calculated by the asymptotic formula given in Corollary 1. The age and gender variables show a strongly significant effect by these three methods with p-values close to zero, while resting blood pressure and serum cholesterol show a very weak effect by the three methods with large p-values. Moreover, by the MCP and SCAD methods, the effects of fasting blood sugar indicator and resting electrocardiographic results become more significant than the results by the OLS method. This result indicates that by recovering the hidden heterogeneous structure of the data, it helps us identify useful variables which may have effects on the response. We also calculate the coefficient of determination  $R^2$ , and obtain  $R^2 = 0.667, 0.704$  and  $0.109$  for MCP, SCAD and OLS methods. We see that taking into account the subgroup structure leads to a significant improvement of the model fitting. Next we apply the Gaussian mixture model-based method to this dataset for cluster analysis. As described in Example 4 of the simulation section, we apply the MCLUST to the pseudo observations  $y_i - \mathbf{x}_i^T \hat{\beta}$ , where  $\hat{\beta}$  is obtained from the OLS. As a result, two subgroups are identified. For the real data, since

the true underlying cluster structure is unknown, we cannot use the external criterion, Rand Index measure, to evaluate and compare different methods. Instead, we use the internal criterion, the Davies–Bouldin index, to assess the quality of clustering algorithms, which is calculated by the formula:  $DB = \hat{K}^{-1} \sum_{k=1}^{\hat{K}} \max_{k' \neq k} ((\sigma_k + \sigma_{k'}) / d(c_k, c_{k'}))$ , where  $\hat{K}$  is the estimated number of clusters,  $c_x$  is the centroid of cluster  $x$ ,  $\sigma_x$  is the average distance of all observations  $y_i - \mathbf{x}_i^T \hat{\boldsymbol{\beta}}$  in cluster  $x$  to centroid  $c_x$ , and  $d(c_k, c_{k'})$  is the distance between centroids  $c_k$  and  $c_{k'}$ . The clustering algorithm that has the smallest Davies–Bouldin index is considered the best algorithm based on this criterion. The Davies–Bouldin index values for MCP, SCAD and MCLUST are 0.469, 0.467, and 0.506, respectively, so that the MCP and SCAD outperform the MCLUST based on this criterion.

## 7 Discussion

The model (1) is related to the Neyman-Scott models (Neyman and Scott (1948)). In the terminology of Neyman and Scott, the  $\mu_i$ 's in (1) are called incident parameters. In the literature, such parameters are usually treated as nuisance parameters, while the main interest lies in estimating the common parameter such as  $\{\boldsymbol{\beta}, \sigma^2\}$  in (1) based on panel data (Lancaster (2000)). The problem we consider here is different and we use the  $\mu_i$ 's to represent latent heterogeneity in the observations for the purpose of conducting subgroup analysis. Also we do not assume that panel data are available, so model (1) is not identifiable without a constraint on the parameter space such as the subgroup structure considered in the present paper.

It is also possible to adopt a random effects model approach by taking the  $\mu_i$ 's in (1) as random variables from a mixture distribution. Then the estimation and inference can be carried out using a likelihood-based method. The main difficulty in applying this approach is that it requires specifying the number of subgroups, the parametric form of the mixture distribution, and an assumption on the error distribution. It is worth noting that the choice of the number of groups is always crucial in mixture model-based methods. Different methods on this topic have been proposed in the literature. Among them, the Bayesian model selection criteria (Fraley and Raftery (1998)) are widely used, and the gap statistic proposed

in Tibshirani et al (2001) is also an important tool. Our proposed penalized method provides another possible approach to automatically estimate the number of groups with reliable theoretical properties. By using the MCLUST, our simulation studies show that the clustering accuracy is improved by using the proposed penalized method to select the number of groups compared to the BIC.

In our theoretical results, we allow  $p$ , the dimension of the regression parameter  $\beta$ , to diverge with  $n$ , but require it to be smaller than  $n$ . For models and data with  $p > n$ , a sparsity condition needs to be imposed on  $\beta$  and an additional penalty term to enforce the sparsity is required. Computationally, we can still derive an algorithm within the framework. However, much extra effort is needed to establish the theoretical properties of the estimators in this high-dimensional setting. This is an interesting and challenging technical problem and deserves further investigation, but is beyond the scope of this paper.

The proposed method can be extended to other models including the generalized linear models and regression models for censored survival data. Although these extensions appear to be conceptually straightforward, it is a nontrivial task to develop computational algorithms and establish theoretical properties in these more complicated models.

## References

- Banfield, J. D. and Raftery, A. E. (1996). Model-based Gaussian and non-Gaussian clustering. *Biometrics*, 49, 803-821.
- Besag, J. (1974). Spatial interaction and the statistical analysis of lattice systems. *Journal of the Royal Statistical Society, Series B*, 36, 192-236.
- Bertsekas, D. P. (2003). *Nonlinear Programming*, Athena Scientific, 2nd edition. 109, 475-494.
- Bondell, H. D. and Reich, B. J. (2008). Simultaneous regression shrinkage, variable selection, and supervised clustering of predictors with oscar. *Biometrics*, 64, 1151-123.
- Boyd, S. and Parikh, N. and Chu, E. and Peleato, B. and Eckstein, J. (2011). Distributed

- optimization and statistical learning via the alternating direction method of multipliers. *Foundations and Trends in Machine Learning*, 3, 1122.
- Chaganty, A. T. and Liang, P. (2013). Spectral experts for estimating mixtures of linear regressions. *Proceedings of the 30th International Conference on Machine Learning*, 28, 10401048.
- Chi, E. C. and Lange, K. (2014). Splitting methods for convex clustering. *Journal of Computational and Graphical Statistics*, forthcoming.
- Everitt, B. and Hand, D. J. (1981). *Finite Mixture Distributions*, New York, Chapman and Hall.
- Fan, J. and Li, R. (2001). Variable selection via nonconcave penalized likelihood and its oracle properties. *Journal of the American Statistical Association*, 96, 1348-1360.
- Fraley, C. and Raftery, A. E. (2002). Model-based clustering, discriminant analysis, and density estimation. *Journal of the American Statistical Association*, 97, 611-631.
- Fraley, C. and Raftery, A. E. (1998). How many clusters? Which clustering method? Answers via model-based cluster analysis. *The Computer Journal*, 41, 578-588.
- Guo, F. J. and Levina, E. and Michailidis, G. and Zhu, J. (2010). Pairwise variable selection for high-dimensional model-based clustering. *Biometrics*, 66, 793-804.
- Hastie, T. and Tibshirani, R. (1996). Discriminant analysis by Gaussian mixtures. *Journal of the Royal Statistical Society, Series B*, 58, 155176.
- Ke, T. and Fan, J. and Wu, Y. (2010). Homogeneity in regression. *Journal of the American Statistical Association*, 110, 175-194.
- Lancaster, T. (2000). The incident parameter problem since 1948. *Journal of Econometrics*, 95, 391-413.
- Lauer, M. S. and Francis, G. S. and Okin, P. M. and Pashkow, F. J. and Snader, C. E. and Marwick, T. H. (1999). Impaired chronotropic response to exercise stress testing as a predictor of mortality. *Journal of the American Medical Association*, 281, 524-529.

- McNicholas, P. D. (2010). Model-based classification using latent Gaussian mixture models. *Journal of Statistical Planning and Inference*, 140, 1175-1181.
- Neyman, J. and Scott, E. L. (1948). Consistent estimation from partially consistent observations. *Econometrica*, 16, 1-32.
- Rand, W. M. (2010). Objective criteria for the evaluation of clustering methods. *Journal of the American Statistical Association*, 66, 846-850.
- Schwarz, C. (1978). Estimating the dimension of a model. *The Annals of Statistics*, 6, 461-464.
- Shen, J. and He, X. (2015). Inference for subgroup analysis with a structured logistic-normal mixture model. *Journal of the American Statistical Association*, 110, 303-312.
- Shen, X. and Huang, H. C. (2010). Grouping pursuit through a regularization solution surface. *Journal of the American Statistical Association*, 105, 727-739.
- Tibshirani, S. and Saunders, M. and Rosset, S. and Zhu, J. and Knight, K. (2005). Sparsity and smoothness via the fused lasso. *Journal of Royal Statistical Society, Series B*, 67, 911-940.
- Tibshirani, R. and Walther, G. and Hastie, T. (2001). Estimating the number of clusters in a dataset via the Gap statistic. *Journal of the Royal Statistical Society: Series B*, 63, 411-423.
- Tseng, P. (2001). Convergence of a block coordinate descent method for nondifferentiable minimization. *Journal of Optimization Theory and Applications*, 109, 475-494.
- Wang, H. and Li, R. and Tsai, C. L. (2007). Tuning parameter selectors for the smoothly clipped absolute deviation method. *Biometrika*, 94, 553-568.
- Wang, H. and Leng, C. (2009). Shrinkage tuning parameter selection with a diverging number of parameters. *Journal of Royal Statistical Society, Series B*, 71, 671-683.



Wei, S. and Kosorok, M.R. (2013). Latent supervised learning. *Journal of the American Statistical Association*, 108, 957-970.

Zhang, C. (2010). Nearly unbiased variable selection under minimax concave penalty. *The Annals of Statistics*, 38, 894-942.

Zenger, C. (1991). *Sparse Grids*, Vieweg, Braunschweig, Notes on Numerical Fluid Mechanics.